Photoproduction and electroproduction of nucleon resonances in point form relativistic quantum mechanics

Y. B. Dong
CCAST (World Laboratory), Post Office Box 8730, Beijing 100080, China and
Institute of High Energy Physics, The Chinese Academy of Sciences, Beijing 100049, China
(Received 28 January 2005; published 21 September 2005)

We employ point form relativistic quantum mechanics to calculate the photoproduction and electroproduction of nucleon resonances. Both the transverse and longitudinal transition amplitudes are computed based on the constituent quark model within the relativistic framework. The obtained results are compared with the calculations of the nonrelativistic approach and of the hypercentral potential model. Relativistic effects and discrepancies among the models are discussed.

DOI: 10.1103/PhysRevC.72.035204 PACS number(s): 12.39.−x, 13.40.Em, 14.20.Gk, 25.20.Lj

I. INTRODUCTION

We know that the nonrelativistic constituent quark model has been employed to study low-energy hadronic phenomena for a long time. The discussion of photoproduction and electroproduction amplitudes of low-lying nucleon resonances with this approach is one of the most interesting topics since knowledge of those amplitudes is closely related to nonperturbative QCD and can provide detailed information about the structure of the nucleon. It is believed that new data of nucleon structure functions in the resonance region and of nucleon resonance transition amplitudes can provide a test for different model predictions. Even though there are many calculations in the literature, most of them are done within the nonrelativistic framework and consider relativistic corrections to the electromagnetic transition operators and to the nucleon and resonance wave functions [1–3]. It has been extensively discussed that the conventional long-wavelength approximation in the reduction of electromagnetic transition operators in the nonrelativistic constituent quark model (see Ref. [2]) is not valid if the virtuality of the photon Q^2 is around 1 GeV^2. Moreover, the heavier the resonance is, the smaller is the valid range of the long-wavelength approximation. Thus, calculated transition amplitudes are expected to be valid in a region of rather small Q^2. It should be stressed that Lorentz covariance is apparently lacking in those phenomenological calculations [1–3]. Recently, the measurements of quark-hadron duality indicate that the duality of the nucleon structure function F_2 may occur in the moderate-Q^2 region ($\sim$1 GeV^2) [4,5]. To understand the quark-hadron duality and the nucleon structure functions in the resonance region, we need to have a correct description of the nucleon electromagnetic transition amplitudes in this moderate-Q^2 region.

In 1949, Dirac [6] first proposed three equivalent forms of relativistic dynamics: the instant form, the light-front form, and the point form. In the instant form of relativistic quantum mechanics, the interactions are involved in P_0 (the time component of the four-momentum) and in the Lorentz boost operators J_{01}, J_{02}, and J_{03}. Therefore, the main difficulty of this form is that the manifest Lorentz covariance is lost by construction because the three Lorentz boost operators contain the interactions. In the point form, however, all the components of the four-momentum $P_\mu(\mu = 0, 1, 2, 3)$ are associated with the interactions. They are the Hamiltonians of the system. Other dynamical operators, such as angular momentum and Lorentz boost operators, are interaction free. Thus, the advantage of the point form is that all the Lorentz transformations remain purely kinematic and the theory is manifestly Lorentz covariant. The instant and light-front forms have become rather popular in the past several decades and most of the calculations are based on these two frameworks. The point form framework has been discussed by Keister and Polyzou [7] in 1991 and has recently been carefully and systematically studied by Klink [8]. It was also employed in the calculations of nucleon form factors [9], nucleon resonance strong decays [10], and some other aspects of hadron physics [11,12]. The results of the point form in the literature show the importance of the relativistic description of the system. Particularly, when the momentum transfer Q^2 is at a moderate region of $\sim$1 GeV^2, the differences between the results of the nonrelativistic calculation and those of the fully relativistic point form are evident. It is found, in the calculation of the proton electromagnetic and axial-vector form factors [9], that the point form relativistic description always reduces to the theoretical estimates of the nonrelativistic constituent quark model. In addition, the strong decay widths predicted by the point form [10] are remarkably different from the nonrelativistic constituent quark model calculations. So far, how well the point form relativistic quantum mechanics aids in our understanding of hadron properties is still under investigation [12].

In this work, the point form relativistic quantum mechanics will be employed to calculate invariant electromagnetic transverse and longitudinal transition amplitudes of low-lying nucleon resonances. Moreover, the results of the nonrelativistic framework in two reference frames—the conventional Breit frame and the known equal velocity reference (EVR) frame [13]— will be shown for comparison. It is expected that there are remarkable differences between electromagnetic transition amplitudes of the nonrelativistic framework and those of the relativistic point form one.

This work is organized as follows. In Sec. II, we will briefly present the formulations of the transition amplitudes in the point form relativistic quantum mechanics. Section III will show our calculations and results and other discussion. Conclusions will be given in Sec. IV.

II. FORMULATIONS IN POINT FORM

In this section, we briefly show the point form formulations. In the point form relativistic quantum mechanics, one usually uses the Bakamjian-Thomas method [14] by putting the interactions into a mass operator $\hat{M}$ to construct the interacting four-momentum operator P_μ. In this way, the mass operator $\hat{M}$ can be divided into two parts. One is the free mass operator $\hat{M}_{\rm fr}$ without any interactions and the other is the interacting mass operator $\hat{M}_{\rm int}$. The four-momentum P_μ is related to the mass operator by

$$P^\mu = \hat{M}\hat{V}^\mu_{\rm fr}, \tag{1}$$

where the free four-velocity operator $\hat{V}^\mu_{\rm fr}$ is not affected by the interactions. According to the commutation relations satisfied by the operators of the dynamical system and according to the fact that P^μ is a Lorentz vector, one gets $[V^\mu_{\rm fr}, \hat{M}] = 0$ and $\hat{M}$ is a Lorentz scalar. Thus, the eigenstates of the four-momentum operator P^μ are the eigenstates of both the mass and the velocity operators. In the center-of-mass frame of the system, we can obtain the wave functions of the three-quark system by solving a semirelativistic Schrödinger equation (wherein the nonrelativistic kinetic energy operator is replaced by the semirelativistic one including positive energy only). Those wave functions are the eigenstates of the mass operator with interactions. Since in the point form the Lorentz transformations remain purely kinematic, the so-called velocity state is usually introduced as follows:

$$\begin{aligned}|v;\vec{k}_1,\vec{k}_2,\vec{k}_3;\mu_1,\mu_2,\mu_3\rangle &= U_{B(v)}|k_1,k_2,k_3;\mu_1,\mu_2,\mu_3\rangle \\ &= \prod_{i=1}^{3} D^{1/2}_{\sigma_i\mu_i}[R_W(k_i,B(v))]|p_1,p_2,p_3;\sigma_1,\sigma_2,\sigma_3\rangle,\end{aligned} \tag{2}$$

where $k_i, i = 1{-}3$ are the quark momenta in the center-of-mass frame ($\sum_i \vec{k}_i = 0$). $B(v)$ is a Lorentz boost with four-velocity v. In Eq. (2) $p_i = B(v)k_i$, and $U_{B(v)}$ is a unitary representation of $B(v)$. $D^{1/2}(R_W)$ is the spin-1/2 representation matrix of the Wigner rotation $R_W(k_i, B(v)) = B^{-1}(B(v)k_i)B(v)B(k_i)$ [15]. A detailed discussion of the transformation properties of the velocity states has been given in Ref. [8]. It has been proved that all Wigner rotations of a canonical boost of a velocity state are the same. Therefore, the spins can thus be coupled together to a total spin state as in the nonrelativistic framework as well as in the center-of-mass frame. This is the practical advantage of using the velocity state in the point form relativistic mechanics.

To calculate photoproduction and electroproduction amplitudes of a nucleon resonance, we simply employ the point form spectator approximation in the electromagnetic interaction, as developed in Refs. [8] and [9]. Here, it should be mentioned that the momentum transferred to the total nucleon is different from the momentum transferred to the struck constituent. The conserved electromagnetic current operator contains both the one-body current and the dynamically determined current [16]:

$$J_\mu := j^1_\mu + j^{\rm DD}_\mu. \tag{3}$$

The one-body electromagnetic current j^1_μ in the point form spectator approximation has the usual form of a pointlike Dirac particle,

$$\langle p'_i,\lambda'_i|j^1_\mu|p_i,\lambda_i\rangle = e_i\bar{u}(p'_i,\lambda_i)\gamma_\mu u(p_i,\lambda_i), \tag{4}$$

where $u(p_i,\lambda_i)$ is the Dirac spinor with momentum p_i and spin λ_i for the ith struck quark. The matrix element of the dynamically determined current is [16]

$$\langle p',\lambda'_i|j^{\rm DD}_\mu|p,\lambda\rangle = -\frac{q_\mu + q^\perp_\mu}{q^2}q^\nu\langle p,\lambda'_i|j^1_\nu|p,\lambda\rangle, \tag{5}$$

where q_μ is the four-momentum of the incoming photon and $q^\perp_\mu$ is a four-vector perpendicular to q and is determined by the requirement that there should be no pole at $q^2 = 0$. It is clear that the dynamically determined current does not affect the transverse current [16]. Moreover, the gauge-invariant constraint condition $q^\mu J_\mu = 0$ is satisfied.

In fact, the electromagnetic four-momentum $P^\mu_{\rm em}$ of the relativistic point form has been discussed in Ref. [8]. $P^\mu_{\rm em}$ is obtained by integrating $J^\nu(x)A_\nu(x)$ [where $A_\nu(x)$ is the photon field] over a forward hyperboloid [$x^\mu x_\mu = (c\tau)^2, x_0 > 0$, where c is the speed of light]:

$$\begin{aligned}P^\mu_{\rm em} &= \int d^4x\delta(x\cdot x - (c\tau)^2)x^\mu\theta(x^0)J^\nu(x)A_\nu(x) \\ &= \int \frac{d^3x}{\sqrt{(c\tau)^2 + \vec{x}\cdot\vec{x}}}\begin{pmatrix} c\tau \\ \vec{x}\end{pmatrix}^\mu J^\nu(x)A_\nu(x),\end{aligned} \tag{6}$$

where τ is a constant. Here, we simply use $P^0_{\rm em} = \int d^3x J^\nu(x)A_\nu(x)$ (in the nonrelativistic limit: $c \to \infty$).

We can directly calculate the transition amplitudes by using the same approach as in the calculation of resonance strong decays in the point form [10]. We know that the transverse (longitudinal) transition amplitude is the matrix element of the transverse (longitudinal) photon and quark interaction of $H^T_{\rm em}$ ($H^L_{\rm em}$). In the fully relativistic point form, the results of the amplitudes are frame independent. However, in the nonrelativistic constituent quark model, the results are reference frame dependent because the lack of Lorentz covariance. In that approach, the electromagnetic transition amplitudes of the nucleon resonances are usually studied in the conventional Breit and EVR frames [13]. In Table I, we

TABLE I. Incoming photon four-momentum $q^\mu = (\omega, 0, 0, q)$, and the four-momenta of the initial nucleon (P_i) and of the final resonance (P_f) in the Breit and EVR frames. M_N and M_X are the masses of the nucleon and of the final resonance X, and Q^2 is associated with the four-momentum transfer to the nucleon, $Q^2 = -(\omega^2 - \vec{q}^2)$ (here, we select $\vec{q} \parallel \hat{z}$).

Quantities	Breit frame	Equal velocity reference frame
q	$\sqrt{\frac{(Q^2+M_N^2+M_X^2)^2-4M_N^2M_X^2}{Q^2+2(M_N^2+M_X^2)}}$	$(M_N+M_X)\sqrt{\frac{Q^2+(M_X-M_N)^2}{4M_NM_X}}$
ω	$\frac{M_X^2-M_N^2}{\sqrt{Q^2+2(M_X^2+M_N^2)}}$	$(M_X-M_N)\sqrt{\frac{Q^2+(M_X+M_N)^2}{4M_NM_X}}$
P_i	$(\sqrt{M_N^2+\frac{q^2}{4}}, 0, 0, -\frac{q}{2})$	$(\frac{M_N\omega}{M_X-M_N}, 0, 0, -\frac{M_Nq}{M_X+M_N})$
P_f	$(\sqrt{M_X^2+\frac{q^2}{4}}, 0, 0, \frac{q}{2})$	$(\frac{M_X\omega}{M_X-M_N}, 0, 0, +\frac{M_Xq}{M_X+M_N})$
$q^\perp$	$(q, 0, 0, \omega)$	$(q, 0, 0, \omega)$

explicitly list incoming photon momentum and energy, and the four-momentum of the initial nucleon or final resonance in the Breit and EVR frames [13], respectively. In addition, the four-vector $q^\perp$ perpendicular to q is also given in Table I.

It should be stressed that the results in the fully relativistic point form description are frame independent. For $H^T_{\rm em}$, this is because the initial and final momenta $P_i = M_N V_i$ and $P_f := M_X V_f$, and the initial and final velocities V_i and V_f, are in the z direction in both the Breit and EVR frames. We have $U^\dagger(\Lambda) J_x(0) U(\Lambda) = J_x(0)$, where Λ is the Lorentz transformation relating to the two frames (Breit and EVR), and $U(\Lambda)$ is the unitary representation of the Lorentz transformation Λ with $U^\dagger(\Lambda)U(\Lambda) = 1$. Thus, for transverse amplitudes, the predictions of the fully relativistic point form framework are reference frame independent. Here, the amplitude is

$$
\begin{aligned}
A_{\mu',\mu} &= \xi \langle f, \mu' | H^T_{\rm em} | i, \mu \rangle = -\sqrt{\frac{2\pi\alpha_E}{\omega}} \xi \langle f, \mu' | \vec{J} \cdot \vec{\epsilon} | i, \mu \rangle \\
&= 3\xi \int \frac{d^3p_1}{(2\pi)^3} \frac{d^3p_2}{(2\pi)^3} \frac{d^3p_3}{(2\pi)^3} \frac{d^3p'_1}{(2\pi)^3} \frac{d^3p'_2}{(2\pi)^3} \frac{d^3p'_3}{(2\pi)^3} \\
&\quad \times (2\pi)^6 \delta^3(\vec{k}_1 + \vec{k}_2 + \vec{k}_3) \delta^3(\vec{k}'_1 + \vec{k}'_2 + \vec{k}'_3) \\
&\quad \times \psi^*_{J',\mu'}(\vec{p}'_\rho, \vec{p}'_\lambda; \mu'_1, \mu'_2, \mu'_3) \psi_{1/2,\mu}(\vec{p}_\rho, \vec{p}_\lambda; \mu_1, \mu_2, \mu_3) \\
&\quad \times D^{*1/2}_{\lambda'_3\mu'_3}[R_W(k'_3, B(v_{\rm out}))] \langle p'_3, \lambda'_3 | - \sqrt{\frac{2\pi\alpha_E}{\omega}} \vec{J}_+ | p_3, \lambda_3 \rangle D^{1/2}_{\lambda_3\mu_3}[R_W(k_3, B(v_{\rm in}))] \\
&\quad \times D^{1/2}_{\mu'_1\mu_1}[R_W(k_1, B^{-1}(v_{\rm out}) B(v_{\rm in}))] D^{1/2}_{\mu'_2\mu_2}[R_W(k_2, B^{-1}(v_{\rm out}) B(v_{\rm in}))] \\
&\quad \times \delta^3(k'_1 - B^{-1}(v_{\rm out}) B(v_{\rm in}) k_1) \delta^3(k'_2 - B^{-1}(v_{\rm out}) B(v_{\rm in}) k_2),
\end{aligned} \tag{7}
$$

where $\alpha_E = 1/137$. If we choose $\epsilon = -\frac{1}{\sqrt{2}}(0, 1, i, 0)$, then $J_+ = -\frac{1}{\sqrt{2}}(J_x + iJ_y)$. In Eq. (7) $p'_i = B(v_{\rm out}) k'_i$ and $p_i = B(v_{\rm in}) k_i$; μ and μ' are the projections of the angular momenta of the initial nucleon (1/2) and its final resonance (J'), respectively; the two wave functions are the intrinsic wave functions of the initial nucleon and final resonance with the momentum conjugates p_ρ and p_λ of intrinsic Jacobi coordinates; and ξ is the sign of the pionic decay of the resonance. Owing to the symmetry of the wave functions it is sufficient to consider only one case where quark 3 is struck by the incoming photon, while the other two are spectators, and to multiply the results by a factor of 3. The conventional transition amplitude $A_{1/2}$ or $A_{3/2}$ is determined from the matrix element of Eq. (7) by setting the quantum numbers of the initial nucleon (μ) and of the final resonance (μ') to be $-1/2$ and 1/2, or 1/2 and 3/2, respectively.

In a similar way, one can calculate the longitudinal electromagnetic transition amplitude based on the relativistic point form. References [17,18] show the longitudinal amplitude in the nonrelativistic constituent quark model with the relativistic corrections. In this work, the amplitude $S_{1/2}$ is defined in terms of the matrix element of the longitudinal electromagnetic interaction $H^L_{\rm em}$ [19]:

$$
\begin{aligned}
S_{1/2} &= \xi \langle f, \mu' | H^L_{\rm em} | i, \mu \rangle = \xi \langle f, \mu' | \sqrt{\frac{2\pi\alpha_E}{\omega}} \epsilon^L_\mu \cdot J^\mu | i, \mu \rangle \\
&= 3\xi \int \frac{d^3p_1}{(2\pi)^3} \frac{d^3p_2}{(2\pi)^3} \frac{d^3p_3}{(2\pi)^3} \frac{d^3p'_1}{(2\pi)^3} \frac{d^3p'_2}{(2\pi)^3} \frac{d^3p'_3}{(2\pi)^3} \\
&\quad \times (2\pi)^6 \delta^3(\vec{k}_1 + \vec{k}_2 + \vec{k}_3) \delta^3(\vec{k}'_1 + \vec{k}'_2 + \vec{k}'_3) \\
&\quad \times \psi^*_{J',1/2}(\vec{p}'_\rho, \vec{p}'_\lambda; \mu'_1, \mu'_2, \mu'_3) \psi_{1/2,1/2}(\vec{p}_\rho, \vec{p}_\lambda; \mu_1, \mu_2, \mu_3) \\
&\quad \times D^{*1/2}_{\lambda'_3\mu'_3}[R_W(k'_3, B(v_{\rm out}))] \langle p'_3, \lambda'_3 | \sqrt{\frac{2\pi\alpha_E}{\omega}} \frac{\sqrt{Q^2}}{q} J_0 | p_3, \lambda_3 \rangle D^{1/2}_{\lambda_3\mu_3}[R_W(k_3, B(v_{\rm in}))] \\
&\quad \times D^{1/2}_{\mu'_1\mu_1}[R_W(k_1, B^{-1}(v_{\rm out}) B(v_{\rm in}))] D^{1/2}_{\mu'_2\mu_2}[R_W(k_2, B^{-1}(v_{\rm out}) B(v_{\rm in}))] \\
&\quad \times \delta^3(k'_1 - B^{-1}(v_{\rm out}) B(v_{\rm in}) k_1) \delta^3(k'_2 - B^{-1}(v_{\rm out}) B(v_{\rm in}) k_2).
\end{aligned} \tag{8}
$$

where the photon three-momentum is selected to be $\vec{q} \parallel \hat{z}$ [with $q^\mu = (\omega, \vec{q})$ and $\vec{q} = (0, 0, q)$]. This definition of the longitudinal transition amplitude is consistent with that of the transverse transition amplitude in Eq. (7). Usually, the polarization vector of the longitudinal polarized photon is selected to be $\epsilon^L_\mu = (q/\sqrt{Q^2}, 0, 0, \omega/\sqrt{Q^2})$, so that the constraint condition $q^\mu \epsilon^L_\mu = 0$ is satisfied [17,20]. For the longitudinal photon quark vertex, the electromagnetic interaction is, therefore, $H^L_{\rm em} = \epsilon^L_0 J^0 - \epsilon^L_3 J^3$. The gauge-invariant condition $q^\mu J_\mu = 0$ [17,20] gives $\langle f|H^L_{\rm em}|i\rangle = \sqrt{Q^2}/q\langle f|J_0|i\rangle$. Clearly, the longitudinal electromagnetic interaction in Eq. (8) is proportional to $\sqrt{Q^2}$, and it vanishes in the real photon limit $Q^2 = 0$. The interaction $H^L_{\rm em}$ is a Lorentz scalar. Thus, the results of the longitudinal transition amplitude in the fully relativistic point form are frame independent. It should be mentioned that the longitudinal transition amplitude defined in the conventional constituent quark model, as in Refs. [17,21], is

$$S^{\rm non}_{1/2} = \xi\langle f, \mu'|\sqrt{\frac{2\pi\alpha_E}{\omega}}J_0|i, \mu\rangle. \tag{9}$$

It is not a Lorentz invariant amplitude. The two definitions of the longitudinal transition amplitude in Eqs. (8) and (9) are different by a factor of $\sqrt{Q^2}/q$. In addition, the results of Eq. (8) in the nonrelativistic framework are still reference frame dependent owing to the lack of the Lorentz covariance.

Here, we stress that the dynamically determined current [see Eq. (5)] does affect the longitudinal current in the point form. This is because the four-momenta of the system are Hamiltonians. In addition, data for the electromagnetic transition amplitudes from the particle data group (PDG) [22] are $A^N_\lambda(X) \cdot A_{X\to\pi N}/|A_{X\to\pi N}|$. The sign $A_{X\to\pi N}/|A_{X\to\pi N}|$ of the coupling $A_{X\to\pi N}$ is involved in those amplitudes since it cannot be determined in elastic $N\pi$ scattering [23]. Therefore, the phases ξ have to be individually calculated in each model to avoid any confusion in comparing the model calculations with the data, especially in critical cases as for the Roper resonance [21,23]. This means that in a theoretical calculation, both the electromagnetic and pion couplings have to be calculated simultaneously. Ignorance of the pion coupling part might lead to incorrect results for the sign.

III. CALCULATIONS, RESULTS, AND DISCUSSION

In our numerical calculations, the conventional harmonic oscillator wave functions are employed for the nucleon and other nucleon resonances [such as the Roper resonance $P_{11}(1440)$, $S_{11}(1535)$, $D_{13}(1520)$, and $F_{15}(1680)$]. The two parameters in the calculations are selected to be $0.16\,{\rm GeV}^2$ for the harmonic oscillator constant α, and $m_q = M_N/3$ for the quark mass. Thus, the frequency of the harmonic oscillator is about 500 MeV, which is required for the mass spectra of nucleon resonances. Here, for simplicity, we do not consider any configuration mixing effect from hyperfine interactions. In Figs. 1 and 2, our results for the transverse transition amplitudes $A_{1/2}$ and $A_{3/2}$ of the $\Delta(1232)$ resonance are plotted. In the two figures, the data are from the PDG [22] and from the compilation of Kamalov and Yang [24]. The results of the nonrelativistic constituent quark model with relativistic corrections [2] (also without configuration mixing) are also illustrated in the two reference frames where the corrections from the relativistic boost (see Ref. [13]) in the EVR frame is considered.

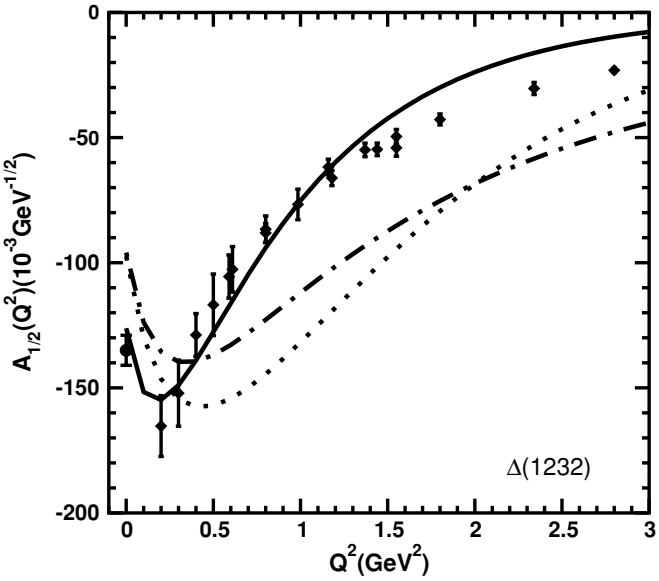

FIG. 1. Electromagnetic transition amplitude $A_{1/2}(Q^2)$ to $\Delta(1232)$. The solid curve represents the results of the point form calculation. The dotted and dotted-dashed curves stand for the calculations of the nonrelativistic constituent quark model with the relativistic corrections in the Breit and EVR frames, respectively. The full circle at real photon point $Q^2 = 0$ is from PDG [22]. The other data denoted by full diamonds are from Ref. [24].

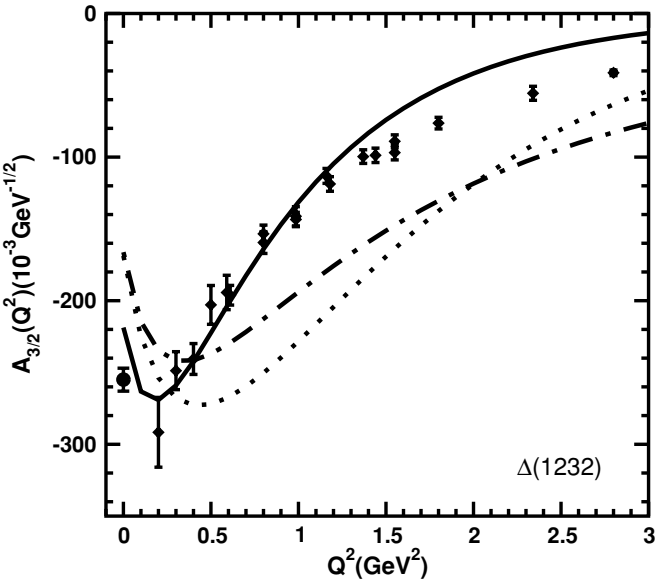

FIG. 2. Electromagnetic transition amplitude $A_{3/2}(Q^2)$ to $\Delta(1232)$. Notation for the curves and symbols are the same as in Fig. 1.

To compare with the nonrelativistic results, we should stress that the nonrelativistic calculation involves some ambiguous assumptions. For example, the fully relativistic boost is not considered, the results for the invariant transverse amplitudes are obviously reference frame dependent, and the long-wavelength approximation in the reduction of the electromagnetic transition operators is not a good approximation if Q^2 is around 1 GeV^2. Figures 1 and 2 clearly show a sizable difference between the relativistic point form description and the two nonrelativistic calculations. One finds that, compared with empirical data, the results of the point form are better than those of the nonrelativistic frame-work, particularly in the region of $Q^2 \sim 1\,\mathrm{GeV}^2$. The absolute magnitudes of the relativistic description, in the region of $Q^2 \geqslant 0.5\,\mathrm{GeV}^2$, are always much smaller than those of the nonrelativistic calculations. This feature is favored by the data and agrees with the calculations of the proton form factors [9]. In addition, our results show that the point form relativistic description provides another way for partially understanding the nonvanishing ratios $E2/M1$ and $S_{1+}/M1$ even though the present framework can only explain a few percent of the whole ratios at the real photon limit ($(-2.5 \pm 0.5)\%$ for $E2/M1$ from PDG [22], for example). Since we did not consider any deformation of the wave function of the $\Delta(1232)$ resonance (configuration mixing), the two ratios in the conventional nonrelativistic constituent quark model with relativistic corrections are exactly zero. In the point form, the estimated values are only about -0.02% for $E2/M1$ and -0.03% for $S_{1+}/M1$ at the real photon point. These two values are about two orders of magnitude smaller than the empirical values. Clearly, configuration mixing and meson cloud effects (as in Refs. [25,26]) are missing in the present calculations. It is expected that those effects play a much more remarkable role in understanding the nonvanishing $E2/M1$ and $S_{1+}/M1$ ratios in the low-Q^2 region.

In Figs. 3–7, the transverse and longitudinal transition amplitudes of the two typical negative-parity nucleon resonances $S_{11}(1535)$ and $D_{13}(1520)$ are shown. In the figures, the numbers of the hypercentral potential model in Refs. [21] and [27] and of the nonrelativistic constituent quark model in the two reference frames (Breit and EVR) are shown for comparison. The data in the figures are taken from the PDG [22] and from the compilations of Refs. [28–30]. In Figs. 4 and 7, we consider the effect of the factor $\sqrt{Q^2}/q$ in the data. The effect is also taken into account in the results of the hypercentral calculations (quoted from Refs. [21] and [27]) in the Breit frame owing to the difference between Eq. (8) and Eq. (9). It has been claimed (see Refs. [21] and [27]) that the hypercentral potential can give a good description for the intermediate-Q^2 behavior of the nucleon resonance transition amplitudes, particularly, their predictions for the amplitude $A_{1/2}(Q^2)$ of $S_{11}(1535)$ in Fig. 3. Here, we also see a reasonable agreement between our point form relativistic calculation and the data. Particularly, the agreement is seen even at a moderate $Q^2 \sim 1 \sim 2\,\mathrm{GeV}^2$. As for the nonrelativistic constituent quark model calculation (see, for example, the dotted curve in Fig. 3), we find that one can modify the model parameters to suppress the calculated result in the real photon point and to get a good fit to the data. However, the results of $A_{1/2}(Q^2)$ at moderate Q^2 will be simultaneously suppressed and the total agreement with the data will become even worse than that of the point form calculation. This feature indicates the advantages of the relativistic point form framework. When the momentum transfer Q^2 is larger than

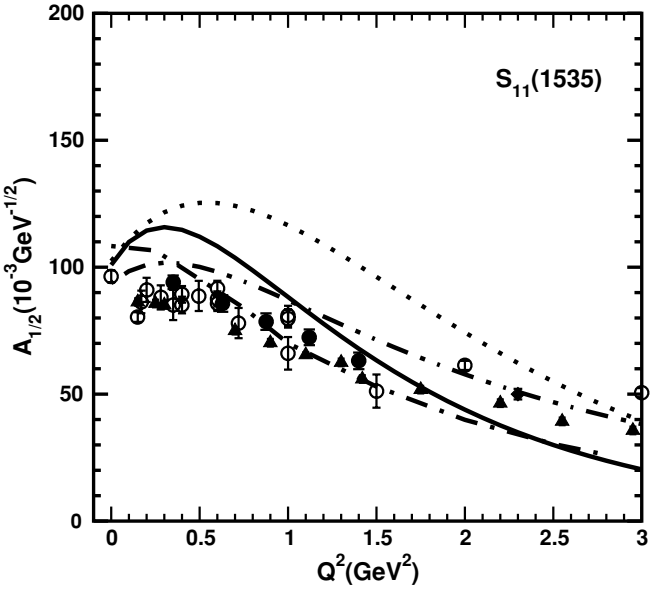

FIG. 3. Electromagnetic transition amplitude $A_{1/2}(Q^2)$ to $S_{11}(1535)$. The double-dotted-dashed curve stands for the results of hypercentral potential model calculations in Refs. [21] and [27]. Other curves are rotated as in Fig. 1. The open circle at the real photon point $Q^2 = 0$ is from PDG [22]. The other data are from Ref. [28].

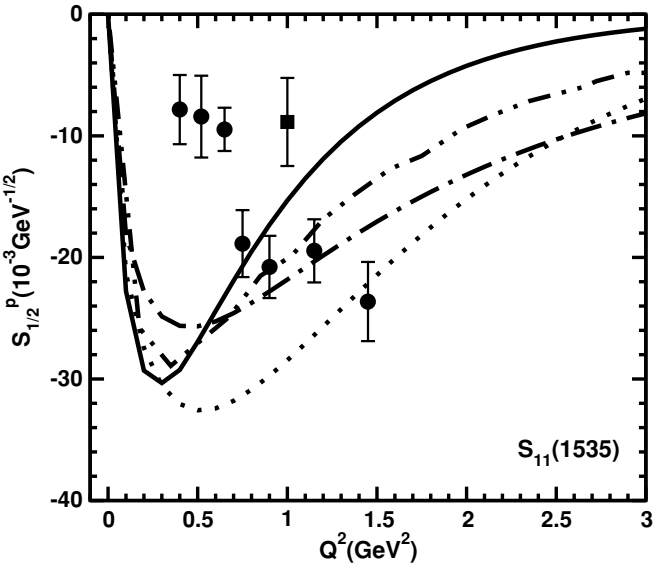

FIG. 4. Electromagnetic longitudinal amplitude $S_{1/2}(Q^2)$ to $S_{11}(1535)$. The solid curve represents the results of the point form calculation. The dotted and dotted-dashed curves stand for the calculations of the nonrelativistic constituent quark model with the relativistic corrections in the Breit and EVR frames, respectively. Other curves and symbols are as in Fig. 3.

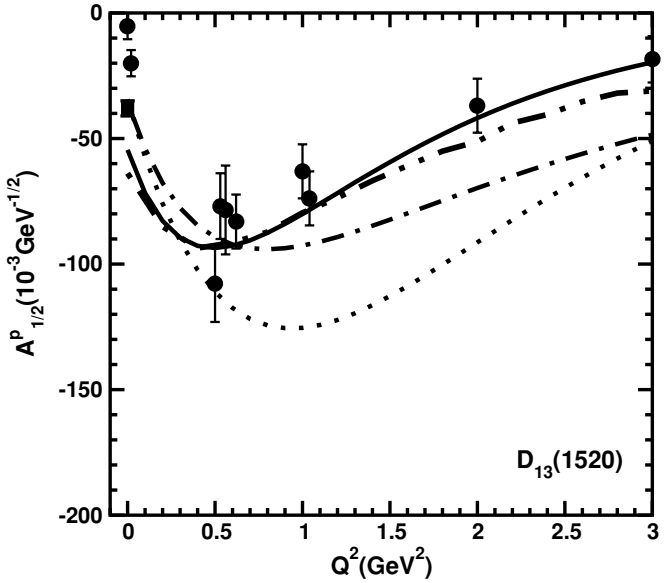

FIG. 5. Electromagnetic transverse transition amplitude $A_{1/2}(Q^2)$ to $D_{13}(1520)$. The full square point at $Q^2 = 0$ is from the recent measurement of Ref. [29]. The other date are from Ref. [28]. Notation for the curves is the same as in Fig. 3.

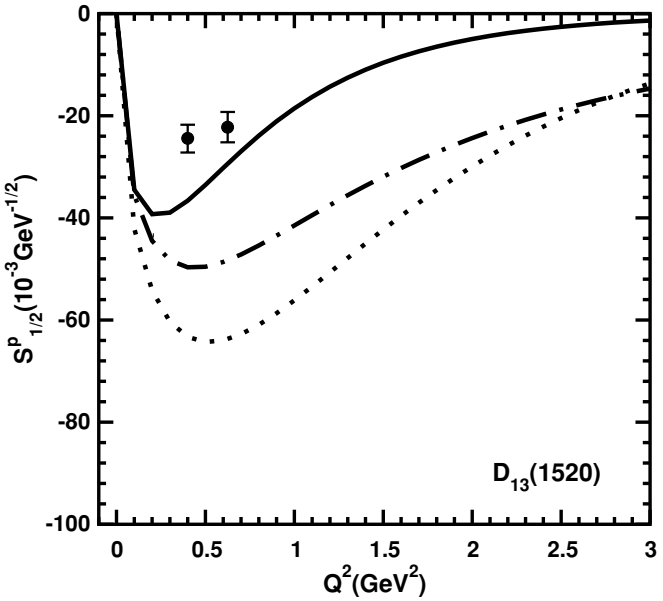

FIG. 7. Electromagnetic longitudinal amplitude $S_{1/2}(Q^2)$ to $D_{13}(1520)$. Notation for the curves and symbols is the same as in Fig. 4. The data are from Ref. [30].

$1\,\text{GeV}^2$, the results of the point form turn out to be less than the values of the hypercentral predictions. This occurs because we are using the harmonic oscillator wave functions [31], which are different from the hypercentral wave functions. In addition, the longitudinal transition amplitudes in this work are related to the matrix elements of the longitudinal photon and quark interaction H^L_{em} [see Eq. (8)]. Thus, the calculated amplitudes are Lorentz invariant in the fully relativistic point form.

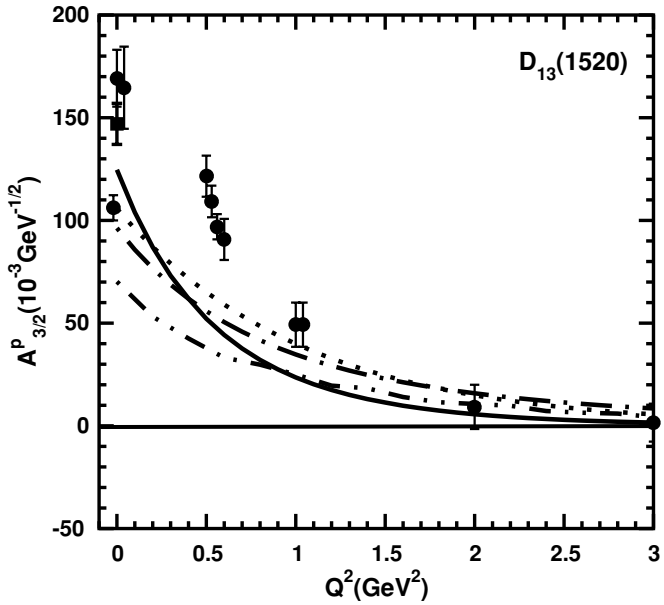

FIG. 6. Electromagnetic transverse amplitude $A_{3/2}(Q^2)$ to $D_{13}(1520)$. Notation for the curves and symbols is the same as in Fig. 5.

For the transition amplitude $A_{1/2}(Q^2)$ of the resonance $D_{13}(1520)$, agreement is also reasonable. The recent data for the helicity amplitudes of $A_{1/2}$ and $A_{3/2}$ of $D_{13}(1520)$ [29] are -0.038 ± 0.003 and 0.147 ± 0.010 (in units of $\text{GeV}^{-1/2}$). These are shown by the full square data points in Figs. 5 and 6 at $Q^2 = 0$. Those new data imply that the empirical value of $A_{1/2}$ increases (in magnitude) and that of $A_{3/2}$ decreases compared to the standard PDG values [22]: -0.024 ± 0.009 and 0.166 ± 0.005. These changes are also favored by theoretical predictions. The fit for the transition amplitude $A_{3/2}(Q^2)$ of the $D_{13}(1520)$ resonance, however, is not as good as that for the $A_{1/2}(Q^2)$ case, particularly, at small- and moderate-Q^2 values. It has been claimed that relativistic kinematics is not responsible for the disagreement [32]. In fact, this situation remains in the hypercentral constituent quark model calculations (see Refs. [21], [27], and [32]). The reason for this discrepancy is the lack of explicit quark-antiquark configurations.

Figures 8–11 show the calculated transverse and longitudinal electromagnetic transition amplitudes of the nucleon resonances $P_{11}(1440)$ and $F_{15}(1680)$ in the point form framework. We see the remarkable discrepancies between the fully relativistic point form framework and the nonrelativistic constituent quark model. Comparing with the data for the $A_{1/2}(Q^2)$ of the Roper resonance, we find that all the calculations of our present model, of the hypercentral model, and of the nonrelativistic constituent quark model with relativistic corrections deviate from measurements in the moderate region of $Q^2 \geqslant 0.5\,\text{GeV}^2$. Our calculation for $S_{1/2}(Q^2)$ of the Roper resonance (see Fig. 9) seems to agree with the data (with the factor $\sqrt{Q^2}/q$ also considered) quantitatively. The magnitudes

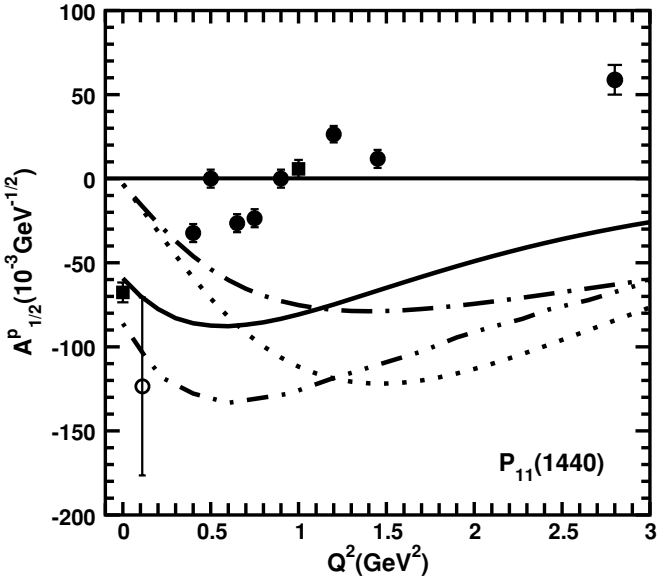

FIG. 8. Electromagnetic transverse amplitude $A_{1/2}(Q^2)$ to the Roper resonance $P_{11}(1440)$. Notation of curves is the same as in Fig. 3. The data are from the compilations of Ref. [21].

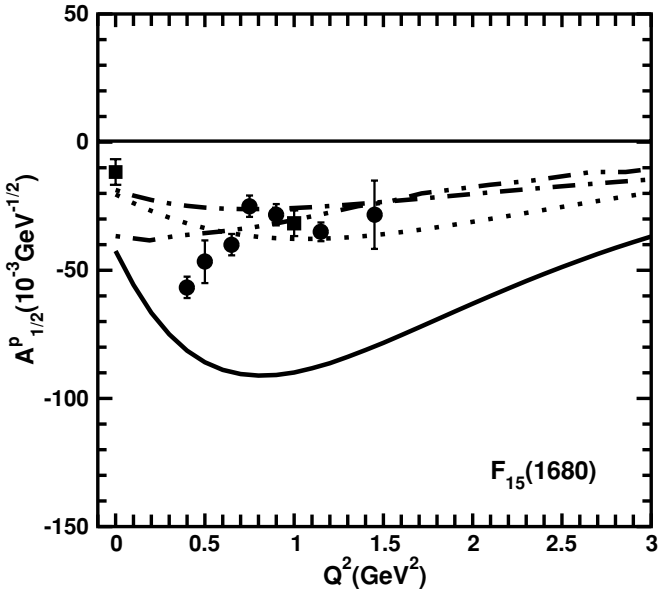

FIG. 10. Electromagnetic transverse amplitude $A_{1/2}(Q^2)$ to $F_{15}(1680)$. Notation of the curves and symbols is the same as in Fig. 3.

of our results are remarkably smaller than the data and the results of the hypercentral potential model. So far, the assignment of the Roper resonance remains controversial. The recent measurement of Jefferson Lab. [30] has almost ruled out the interpretation of this resonance as a q^3G hybrid state [33]. It is argued that the meson cloud effect (not considered here) on the transverse and longitudinal transition amplitudes of the Roper resonance is important [34]. For the transitions of the $F_{15}(1680)$ resonance, we find that our results deviate from the data of $A_{1/2}(Q^2)$ in the moderate-Q^2 region of $\sim$0.4 GeV^2. However, they behave better than the results of the hypercentral model for $A_{3/2}(Q^2)$ compared with the data. In addition, the strengths of the transition amplitudes of the resonance $F_{15}(1680)$ in the real photon limit are short of those in all different model calculations, particularly for $A_{3/2}(Q^2)$.

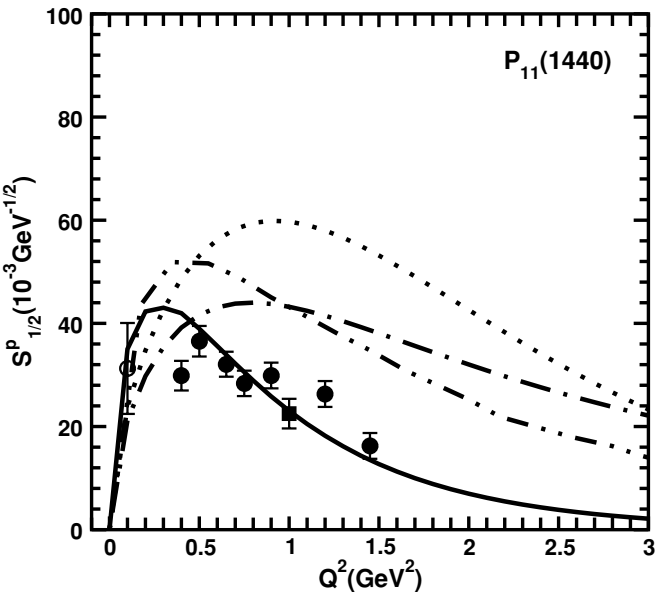

FIG. 9. Electromagnetic longitudinal amplitude $S_{1/2}(Q^2)$ to the Roper resonance $P_{11}(1440)$. Notation of curves and symbols is the same as in Fig. 8 (where the factor $\sqrt{Q^2}/q$ has been considered).

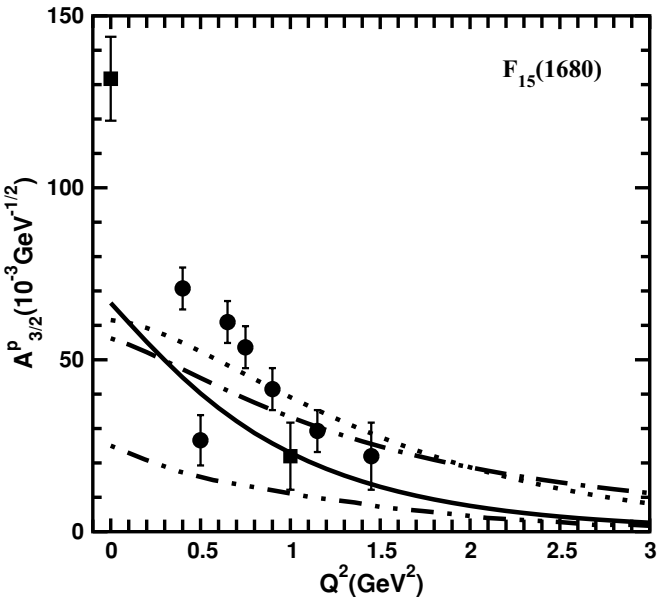

FIG. 11. Electromagnetic transverse amplitude $A_{3/2}(Q^2)$ to $F_{15}(1680)$. Notation for the curves and symbols is the same as in Fig. 3.

IV. CONCLUSIONS

Incorporating the results of the previous calculations for the form factors of the nucleon [8] and of π and ρ mesons [11,12] with this calculation of the transition amplitudes of the nucleon resonances, we conclude that point form relativistic quantum mechanics can provide a convenient way to study hadron properties, particularly the transitions to resonances. Since the relativistic boost is correctly considered in this framework, the results for the Q^2 dependences of the transition amplitudes are expected to be reasonable. This conclusion can be clearly seen from the point form predictions of the transition amplitudes of the $\Delta(1232)$ resonance, as shown in Figs. 1 and 2, and of the $S_{11}(1535)$ in Fig. 3. We find that some of the results calculated in the present point form indicate that the values are smaller in magnitude than those predicted by the conventional constituent quark model when Q^2 increases. This phenomenon has also been seen in proton form factor calculations [9]. Our work shows that reasonable results for the transition amplitudes of $A_{1/2,3/2}(Q^2)$ of the $\Delta(1232)$ resonance and of $A_{1/2}$ of the $S_{11}(1535)$ and $D_{13}(1520)$ resonances can be achieved, but not for the $A_{3/2}$ of $D_{13}(1520)$, the $A_{1/2}(Q^2)$ of the Roper resonance, or of the $F_{15}(1680)$ resonance. Moreover, there are sizable discrepancies between the point form results and the nonrelativistic constituent quark model predictions with relativistic corrections. Because harmonic oscillator wave functions are employed in the two frameworks simultaneously, the discrepancies clearly indicate that relativistic effects need to be correctly taken into account. It should be stressed that the results of both the transverse and the longitudinal transition amplitudes of the fully relativistic point form are reference frame independent. The sizable reference frame dependences show the lack of Lorentz covariance in the nonrelativistic approach.

Finally, we only simply take into account the harmonic oscillator wave functions in our present point form calculations. Other physical ingredients, such as realistic wave functions of the resonances, confinement, the meson cloud, two-body exchange currents, and configuration mixing are not considered at all. Certainly, the predicted results at large Q^2 are not very satisfactory. There is some discussion about the applicability of the point form description [12,35]. It appears that the radius of the bound-state wave function is an important parameter for distinguishing any relativistic effect. Here, much better results are expected if other physical ingredients, such as realistic wave functions, meson cloud effects, and configuration mixing, are consistently included from the beginning. Moreover, in this work, we only use simple three-dimensional harmonic oscillator wave functions. It is argued and expected that the wave functions of the four-dimensional fully relativistic harmonic oscillator [36] and of the hypercentral potential model [32] can provide more reliable results in a relativistic calculation. A systematic study of nucleon resonance transition properties with the hypercentral model in the relativistic point form is in progress.

ACKNOWLEDGMENTS

The author is grateful for discussions with Prof. M. M. Giannini and Dr. E. Santopinto. He also thanks the Department of Physics, Genova University, and the Institute of Theoretical Physics, University of Tuebingen, for their hospitality. Support from the Center of Theoretical Nuclear Physics and Lanzhou National Laboratory's Heavy Ion Accelerator, is also appreciated. This work is supported by the National Natural Science Foundations of China (Grant Nos. 10475088, 10075056, and 90103020), by CAS Knowledge Innovation Project No. KC2-SW-N02, and by the Institute of Theoretical Physics.

[1] F. E. Close and L. A. Copley, Nucl. Phys. **B19**, 477 (1970); F. E. Close and H. Osborn, Phys. Rev. D **2**, 2127 (1970); M. Warns *et al*., Z. Phys. C **45**, 613 (1990); **45** 627 (1990); M. Warns, W. Pfeil, and H. Rollnik, Phys. Rev. D **42**, 2215 (1990); S. Capstick and B. D. Keister, *ibid.* **51**, 3598 (1995); Y. B. Dong, Phys. Rev. C **56**, 702 (1997); R. H. Stanley and H. J. Weber, *ibid*. **52**, 435 (1995).

[2] F. E. Close and Z. Li, Phys. Rev. D **42**, 2194 (1990); Z. Li and F. E. Close, *ibid*. **42**, 2207 (1990).

[3] S. Capstick, Phys. Rev. D **46**, 1965 (1992); **46**, 2864 (1992).

[4] I. Niculescu *et al*., Phys. Rev. Lett. **85**, 1182 (2000); **85**, 1186 (2000).

[5] HERMES Collaboration (A. Fantoni for the Collaboration), Eur. Phys. J. A **17**, 385 (2003); A. Fantoni, N. Bianchi, and S. Liuti, *ibid*. **24s1**, 35 (2005).

[6] P. A. M. Dirac, Rev. Mod. Phys. **21**, 392 (1949).

[7] B. D. Keister and W. N. Polyzou, in *Advanced Nuclear Physics*, edited by J. W. Negele and E. W. Vogt (Pleneum, New York, 1991), Vol. 21, p. 225.

[8] W. H. Klink, Phys. Rev. C **58**, 3587 (1998); W. H. Klink and M. Rogers, *ibid*. **58**, 3605 (1998); W. H. Klink, *ibid*. **58**, 3617 (1998).

[9] L. Ya. Glozman, M. Radici, R. F. Wagenbrunn, S. Boffi, W. Klink, and W. Plessas, Phys. Lett. **B516**, 183 (2001); W. Plessas, S. Boffi, L. Ya. Glozman, W. Klink, M. Radici, and R. F. Wagenbrunn, Eur. Phys. J. A **14**, 17 (2002); R. F. Wagenbrunn, S. Boffi, W. Klink, W. Plessas, and M. Radici, Phys. Lett. **B511**, 33 (2001).

[10] T. Melde, R. F. Wagenbrunn, and W. Plessas, Few Body Syst. Suppl. **14**, 37 (2003); T. Melde, W. Plessas, and R. F. Wagenbrunn, Phys. Rev. C **72**, 015207 (2005).

[11] T. W. Allen and W. H. Klink, Phys. Rev. C **58**, 3670 (1998); T. W. Allen, W. H. Klink, and W. N. Polyzou, *ibid*. **63**, 034002 (2001); A. Krassnigg, W. Schweiger, and W. H. Klink, Few Body Syst. Suppl. **14**, 403 (2003); Phys. Rev. C **67**, 064003 (2003).

[12] B. Desplanques and L. Theussl, Eur. Phys. J. A **13**, 461 (2002); B. Desplanques, L. Theussl, and S. Noguera, Phys. Rev. C **65**, 038202 (2002); A. Amghar, B. Desplanques, and L. Theussl,

Phys. Lett. **B574**, 201 (2003); F. Coester and D. O. Riska, Nucl. Phys. **A728**, 439 (2003); J. He, B. Julia-Diaz, and Y. B. Dong, Phys. Lett. **B602**, 212 (2004).

[13] A. L. Licht and A. Pagnamenta, Phys. Rev. D **2**, 1150 (1970); F. Foster and G. Hughes, Z. Phys. C **14**, 123 (1982).

[14] B. Bakamjian and L. H. Thomas, Phys. Rev. **92**, 1300 (1953); W. H. Klink, Nucl. Phys. **A716**, 158 (2003).

[15] S. Weinberg, *The Quantum Theory of Fields* (Cambridge University Press, Cambridge, England, 1995).

[16] W. H. Klink, Few Body Syst. **33**, 99 (2003).

[17] Z. P. Li, Y. B. Dong, and W. X. Ma, J. Phys. G **23**, 151 (1997); Y. B. Dong, *ibid*. **23**, 1005 (1997).

[18] P. Stoler, Phys. Rep. **226**, 103 (1993); C. E. Carlson and N. C. Mukhopadhyay, Phys. Rev. D **58**, 094029 (1998).

[19] M. De Sanctis, M. M. Giannini, E. Santopinto, and A. Vassallo, Eur. Phys. J. A **10**, s01, 81 (2004).

[20] S. Boffi, C. Giusti, F. D. Pacati, and Marco Radici, *Electromagnetic Response of Atomic Nuclei* (Clarendon Press, Oxford, 1996).

[21] L. Tiator, D. Drechsel, S. Kamalov, M. M. Giannini, E. Santopinto, and A. Vassallo, Eur. Phys. J. A **19**, s01, 55 (2004).

[22] Particle Data Group, Eur. Phys. J. C **15**, 1 (2000).

[23] A. Hosaka, M. Takayama, and H. Toki, Nucl. Phys. **A678**, 147 (2000); S. Capstick and W. Roberts, Prog. Part. Nucl. Phys. **45**, 241 (2000).

[24] S. S. Kamalov and S. N. Yang, Phys. Rev. Lett. **83**, 4494 (1999).

[25] D. H. Lu, A. W. Thomas, and A. G. Williams, Phys. Rev. C **55**, 3108 (1997).

[26] Y. B. Dong, K. Shimizu, and A. Faessler, Nucl. Phys. **A689**, 889 (2001).

[27] M. M. Giannini, E. Santopinto, and A. Vassallo, Nucl. Phys. **A699**, 308 (2002); Prog. Part. Nucl. Phys. **50**, 263 (2003).

[28] V. D. Burkert, arXiv:hep-ph/0207149.

[29] J. Ahrens *et al*. (GDH and A2 Collaboration), Phys. Rev. Lett. **88**, 232002 (2002).

[30] I. G. Aznauryan, V. D. Burkert, H. Egiyan, K. Joo, R. Minehart, and L. C. Smith, Phys. Rev. C **71**, 015201 (2005).

[31] L. Ya. Glozman, W. Plessas, K. Varga, and R. F. Wagenbrunn, Phys. Rev. D **58**, 094030 (1998).

[32] E. Santopinto, F. Iachello, and M. M. Giannini, Eur. Phys. J. A **1**, 307 (1998); M. De Sanctis, E. Santopinto, and M. M. Giannini, *ibid*. **2**, 403 (1998).

[33] Z. Li, Phys. Rev. D **44**, 2841 (1991); Z. P. Li, V. D. Burkert, and Z. J. Li, *ibid*. **46**, 70 (1992).

[34] Y. B. Dong, K. Shimizu, A. Faessler, and A. J. Buchmann, Phys. Rev. C **60**, 035203 (1999); J. Septh, O. Krehl, S. Krewald, and C. Hanhart, Nucl. Phys. **A680**, 328 (2000); O. Krehl, C. Hanhart, C. Krewald, and J. Speth, Phys. Rev. C **62**, 025207 (2000); F. Cardarelli, E. Pace, G. Salme, and S. Simula, Phys. Lett. **B397**, 13 (1997).

[35] W. H. Klink, Few Body Syst. Suppl. **14**, 387 (2003).

[36] Y. S. Kim, Phys. Rev. Lett. **63**, 348 (1989); Y. S. Kim and M. E. Noz, Int. J. Mod. Phys. A **19**, 5435 (2004); Y. S. Kim, arXiv:quant-ph/0304097.